

# Highly Ordered Chevron-Shaped Arrays of Continuous Copper Nano-Dot Lines Formed by Electroless Deposition on Hydrogen-Terminated Si(111) Surfaces<sup>†</sup>

Tomoyuki Nagai,<sup>‡</sup> Akihito Imanishi,<sup>\*,‡,§</sup> and Yoshihiro Nakato<sup>\*,‡,§</sup>

*Division of Chemistry, Graduate School of Engineering Science, Osaka University, Toyonaka, Osaka 560-8531, Japan, and Core Research for Evolutional Science and Technology, Japan Science and Technology Corporation, 4-1-8 Honmachi, Kawaguchi, Saitama 332-0012, Japan*

*Received: August 8, 2006; In Final Form: September 29, 2006*

We have succeeded in forming highly ordered chevron-shaped arrays of continuous copper nano-dot lines by electroless deposition on hydrogen-terminated Si(111) (H–Si(111)) surfaces. Detailed investigations have shown that tiny Cu clusters are preferentially formed at step edges when the electroless deposition is carried out in a deoxygenated neutral aqueous solution of a low Cu<sup>2+</sup> concentration (less than 10  $\mu$ M) with pH  $\cong$  7. This finding was combined with highly ordered step-edge lines on H–Si(111) prepared by the previously reported method of Teflon scratching and NH<sub>4</sub>F etching, which has led to the above success. The present result indicates that designed ordered metal nanowires can be produced by the electroless deposition method, using H–Si(111) surfaces with well-regulated step lines as a substrate.

## Introduction

Nanostructuring at semiconductor surfaces, which constitutes the basis of future hugely integrated and intelligent devices,<sup>1–3</sup> has been attracting keen attention in the field of semiconductor sciences and technologies. Much effort has been done to find and develop new structuring techniques that have a fabrication size significantly smaller than the limit of conventional photolithography.<sup>4–7</sup> Recently, atomic-scale fabrication by use of surface probe microscopes such as scanning tunneling microscopes and scanning near-field optical microscopes<sup>8,9</sup> has been attracting strong attention as a powerful technique for designed and well-controlled nanostructuring, but this technique has a severe limit in that it is not adaptable to mass production, which is inevitably necessary for practical application.

A chemical approach to make use of the self-assembling or self-organizing ability of molecular systems has attracted growing attention because it has a strong merit in that it can be adapted to mass production. In addition, the nanostructures obtained by this method are expected to have high chemical stability and self-restoration ability, contrary to the structures obtained by artificial (physical) techniques such as photolithography and scanning probe microscopy.

Site-selective metal deposition on solid surfaces is a good example of such self-organizing systems. A number of studies have been reported on preferential metal deposition at step edges of solid surfaces. For example, Ohdomari et al.<sup>10</sup> and our group<sup>11</sup> reported that electrodeposition of Cu<sup>10</sup> and Ni<sup>11</sup> on hydrogen-terminated Si(111) (H–Si(111)) surfaces produced continuous nano-dot lines of respective metals along atomic step lines composed of dihydride Si sites. However, Munford et al. reported<sup>12</sup> that the electrodeposition of Au on the H–Si(111)

surfaces from an alkaline solution produced continuous nano-dot lines along monohydride step edges at a sufficiently negative electrode potential. The formation of nanowires has also been studied by the electroless deposition method. Homma et al. reported<sup>13</sup> that the electroless deposition of Cu occurred preferentially at step edges of the H–Si(111) surface, though the Cu atoms in this work did not form continuous nano-dot lines but dots. Tokuda et al. also studied<sup>14,15</sup> the electroless deposition of Cu on Si(111). They reported<sup>14</sup> that, when a deoxygenated water containing 100 ppb Cu<sup>2+</sup> was used as the deposition solution, Cu nanowires were produced along step edges on a water-etched (non-hydrogen-terminated) Si(111) surface, though only Cu dots were deposited on the H–Si(111) surface.

From these reported studies, we can expect that metal nanowires (or continuous nano-dot lines) with regulated arrangements can be fabricated by electroless deposition through controlling the surface step structures as well as the metal deposition conditions. Recently, we reported<sup>16,17</sup> a novel method to control the step-edge lines at the H–Si(111) surface in a highly ordered manner. The key was to combine surface scratching with Teflon tweezers and chemical etching with NH<sub>4</sub>F. The Teflon scratching produced nano-lines of scratch-induced damage at the Si surface, which acted as a stopper for the NH<sub>4</sub>F etching and led to the formation of highly ordered step-edge lines.<sup>16,17</sup>

In the present study, the H–Si(111) surfaces with highly ordered step-edge lines, prepared by the above scratching and etching method, were used as a substrate for the electroless deposition of continuous Cu nano-dot lines. Detailed investigations on the influences of the Cu<sup>2+</sup> concentration, the solution pH, and the step structure (monohydride or dihydride) have revealed that the size, shape, and density of deposited Cu in general drastically changes with variation of these parameters. On the basis of the results, we have succeeded in fabricating highly ordered chevron-shaped arrays of continuous Cu nano-dot lines under an appropriate condition.

<sup>†</sup> Part of the special issue "Arthur J. Nozik Festschrift".

<sup>\*</sup> Author to whom correspondence should be addressed. Fax: +81-6-6850-6237. E-mail: nakato@chem.es.osaka-u.ac.jp.

<sup>‡</sup> Osaka University.

<sup>§</sup> Core Research for Evolutional Science and Technology, Japan Science and Technology Corporation.

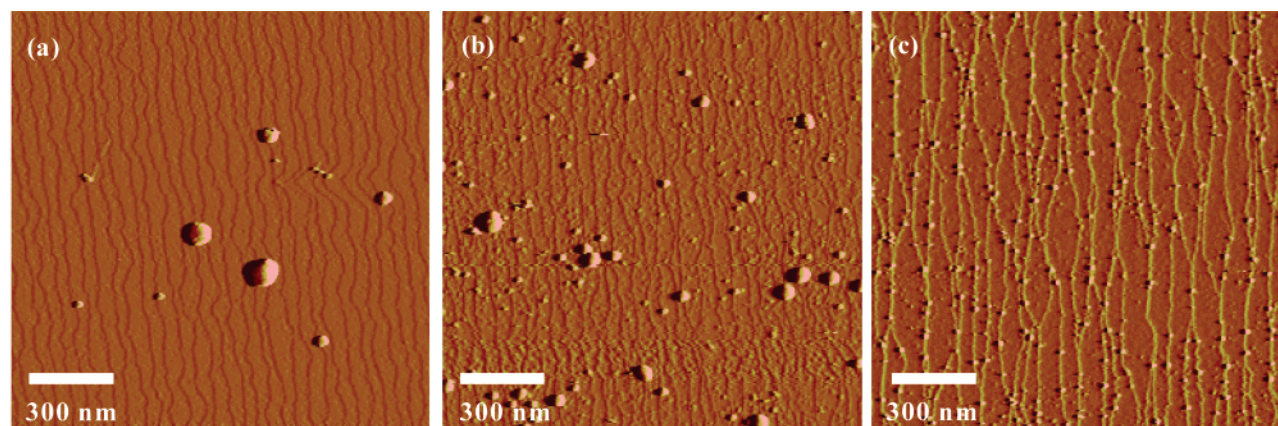


**Figure 1.** AFM images for Cu-deposited H-Si(111) surfaces, obtained by immersing the H-Si(111) wafers in deoxygenated aqueous solutions of (a) 1 mM, (b) 100  $\mu$ M, and (c) 10  $\mu$ M  $\text{CuSO}_4$ .

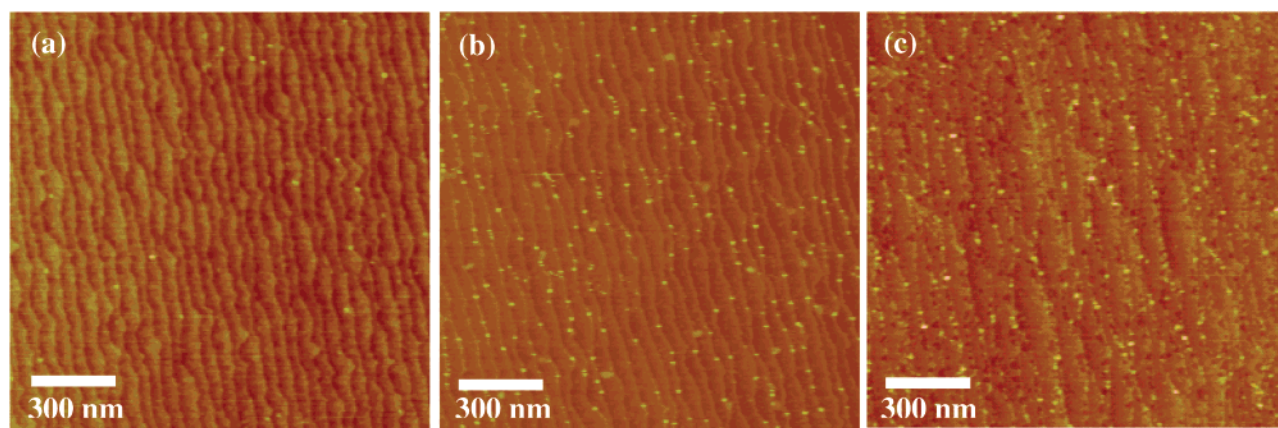


**Figure 2.** AFM images of the Cu-deposited H-Si(111) surfaces obtained by immersion in aqueous solutions of 1  $\mu$ M  $\text{Cu}^{2+}$ , with the pH being changed from (a) 1.9 (1  $\mu$ M  $\text{CuSO}_4$  + 0.05 M  $\text{H}_2\text{SO}_4$ ) to (b) 7.9 (1  $\mu$ M  $\text{CuSO}_4$ ) and to (c) 9.0 (1  $\mu$ M  $\text{CuSO}_4$  + 0.05 M  $\text{NH}_3$ ).

## Experimental Section

Single-crystal n-type Si(111) wafers with a miscut angle of  $0.36 \pm 0.1^\circ$  in the  $\langle 112 \rangle$  direction were obtained from Ferrotec Corporation. The resistivity of the wafers was 1–5  $\Omega$  cm. They were cleaned by the ordinary RCA cleaning method<sup>18</sup> consisting of successive immersion in 98%  $\text{H}_2\text{SO}_4$  + 30%  $\text{H}_2\text{O}_2$  (4:1 in volume) for 10 min, 5% HF for 5 min, 25%  $\text{NH}_4\text{OH}$  + 30%  $\text{H}_2\text{O}_2$  +  $\text{H}_2\text{O}$  (1:1:5 in volume) for 10 min, and 36% HCl + 30%  $\text{H}_2\text{O}_2$  +  $\text{H}_2\text{O}$  (1:1:6 in volume) for 10 min. The wafers were then etched with 5% HF for 5 min and 40%  $\text{NH}_4\text{F}$  for 15 min to obtain atomically flat, hydrogen-terminated Si(111) (H-Si(111)) surfaces.<sup>19</sup>

The samples thus obtained were immersed in aqueous solutions of 0.001–1.0 mM  $\text{Cu}^{2+}$  ( $\text{CuSO}_4$ ) at room temperature (in the presence of the light of fluorescent lamps of a laboratory) for 30 s. The pH of the solutions was controlled by adding an appropriate amount of  $\text{H}_2\text{SO}_4$  or  $\text{NH}_3$ . All the aqueous solutions used were deoxygenated by adding 0.05 M  $(\text{NH}_4)_2\text{SO}_3$  to them.<sup>20–22</sup> Special-grade chemicals were used without further purification. Pure water was obtained by purifying deionized water with a Milli-Q water purification system. The concentration unit, mol  $\text{dm}^{-3}$ , is abbreviated as M in the present paper.

The step structure of the H-Si(111) surface was controlled by scratching Si surfaces with Teflon tweezers in the  $\langle \bar{1}\bar{1}2 \rangle$  direction during the  $\text{NH}_4\text{F}$  immersion.<sup>16</sup> The morphology of Si surfaces was inspected with atomic force microscopy (AFM, Digital Instruments NanoScope IIIa). The AFM images were obtained using a tapping mode under an ex situ conditions with the n-Si surfaces placed in air. The radii of the tips were about

10 nm according to the catalog of a production company (Nanosensors).

## Results

Figure 1 shows AFM images of the Cu-deposited H-Si(111) surfaces, obtained by immersion for 30 s in deoxygenated aqueous solutions of (a) 1 mM, (b) 100  $\mu$ M, and (c) 10  $\mu$ M  $\text{CuSO}_4$  (pH 7.9). Zigzag curves in the images represent step edges, whereas large and small dots refer to deposited Cu particles. The size and density of the dots changed with the concentration of Cu ions in solution, confirming that the dots are composed of Cu. In the case of (a) 1 mM, deposited Cu formed large particles, whose diameter and height were 40–100 and 10–40 nm, respectively. In the case of (b) 100  $\mu$ M, the size of the deposited Cu particles decreased to 20–80 nm in diameter and 3–15 nm in height, though their density increased. In the case of (c) 10  $\mu$ M, the size of the Cu particles became significantly small (10–20 nm in diameter and 2–5 nm in height). These results indicate that the concentration of  $\text{Cu}^{2+}$  ions strongly affects the size and density of the deposited Cu particles. As the concentration of  $\text{Cu}^{2+}$  ions decreased, the deposited particles became smaller, and their density became larger. It should be noted that the deposited Cu particles tend to be located at step edges, in particular under the condition of low  $\text{Cu}^{2+}$  concentrations of 10  $\mu$ M or less. Similar preferential deposition of metals at step edges was reported for the electrodeposition of Au<sup>12</sup> and electroless deposition of Cu.<sup>13,14</sup>

Figure 2 shows the influence of the solution pH on the size and density of the deposited Cu particles. Here the H-Si(111)



surfaces were immersed for 30 s in deoxygenated aqueous solutions with a very low  $\text{Cu}^{2+}$  concentration (1  $\mu\text{M}$ ), the solution pH being changed from (a) 1.9 (1  $\mu\text{M}$   $\text{CuSO}_4$  + 0.05 M  $\text{H}_2\text{SO}_4$ ) to (b) 7.9 (1  $\mu\text{M}$   $\text{CuSO}_4$ ) and to (c) 9.0 (1  $\mu\text{M}$   $\text{CuSO}_4$  + 0.05 M  $\text{NH}_3$ ). In the case of an acidic solution (pH 1.9), Cu deposits were hardly formed at the H–Si(111) surface. In the case of a nearly neutral solution (pH 7.9), continuous Cu nano-dot lines having sizes of 10 nm in diameter and 0.5 nm in height were formed preferentially at step edges, in addition to large-sized Cu dots of 20 nm in diameter and 3 nm in height. In the case of an alkaline solution (pH 9.0), similar Cu clusters to those in part b were formed at the step edges, though the Si surface was considerably etched and the step edges were significantly disarranged.

The above results suggest that the appropriate conditions for producing continuous Cu nano-dot lines along the step edges are: (1) The aqueous solution is deoxygenated, (2) the  $\text{Cu}^{2+}$  concentration is sufficiently low, less than 10  $\mu\text{M}$ , and (3) the solution is neutral with  $\text{pH} \approx 7$ . On the basis of the results, we have next tried to really fabricate well-ordered continuous Cu nano-dot lines, using the H–Si(111) surfaces with highly ordered step edges, produced by the “scratching and etching method” reported in our previous paper.<sup>16</sup> Figure 3a shows an example of the AFM images of the H–Si(111) surfaces with the highly ordered step edges. Vertical inflected thick lines, running nearly in the  $\langle\bar{1}\bar{1}2\rangle$  direction, indicate damage lines induced by the scratching, whereas highly ordered chevron-shaped lines between the damage lines represent step-edge lines produced by the successive 15 min of  $\text{NH}_4\text{F}$  etching. The chevron-shaped step edges obtained were composed of monohydride Si atoms; namely, the steps were monohydride (Si–H) steps.<sup>16,17</sup>

The H–Si(111) surfaces with the chevron-shaped step edges were then immersed in a nearly neutral deoxygenated aqueous solution of low-concentration (1  $\mu\text{M}$ )  $\text{CuSO}_4$  (pH 7.9) for 30 s. Figure 3(b) shows an AFM image of the Cu-deposited H–Si(111) surface thus obtained. Almost all deposited Cu particles were located at the step edges, thus producing highly ordered chevron-shaped arrays of continuous Cu nano-dot lines, whose size is 15 nm in width and 0.5 nm in height. The morphological structure of the Cu deposits in Figure 3b was essentially the same as that in Figure 2b. The inset of Figure 3b shows a three-dimensional diagonal view of the chevron-shaped arrays of continuous Cu nano-dot lines, which clearly indicates that the lines are composed of aligned tiny Cu particles. The scratch-induced damage lines in Figure 3b are bright in color as if Cu were deposited on the lines. However, it is likely that no Cu is deposited, though we have no experimental evidence, because we previously revealed that the scratch-induced lines were composed of chemically inactive compounds.<sup>16,17</sup>

It is well-known that for the Si(111) vicinal surface tilted in the  $\langle\bar{1}\bar{1}2\rangle$  direction the  $\text{NH}_4\text{F}$  etching (without scratching) leads to the formation of the Si surface at which monohydride (Si–H) and dihydride (Si– $\text{H}_2$ ) steps coexist. Figure 4 shows an AFM image for such a  $\text{NH}_4\text{F}$ -etched Si surface, though after the Cu deposition. The Cu metal is deposited as continuous nano-dot lines at both the steps, indicating that the Cu deposition at the step edges occurs regardless of whether they are of monohydride (Si–H) or dihydride (Si– $\text{H}_2$ ). This result indicates that the Cu deposition at the chevron-shaped step edges composed of monohydride (Si–H) (Figure 3b) was basically the same as that at the normal step edges produced by etching without scratching (Figure 2b). In Figure 4, we can see discontinuous parts of the deposited Cu lines here and there. They are probably due to

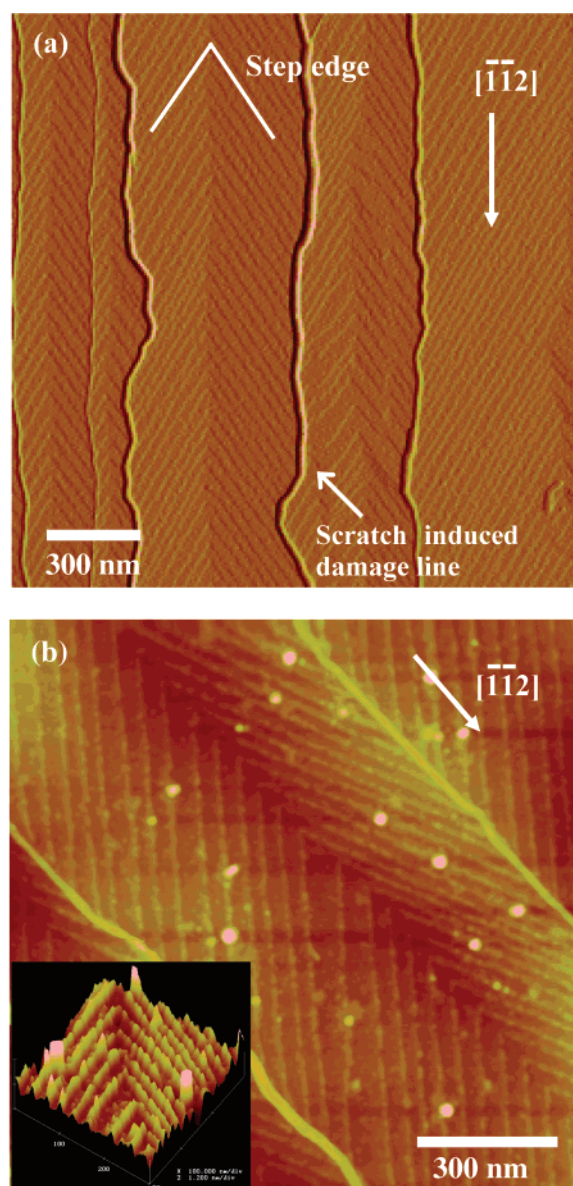


**Figure 3.** (a) AFM image of a H–Si(111) surface with highly ordered chevron-shaped step-edge lines, formed between scratch-induced damage lines. (b) AFM image of a Cu-deposited H–Si(111) surface, in which chevron-shaped arrays of continuous Cu nano-dot lines are produced along the chevron-shaped step-edge lines. The inset is a three-dimensional image of the chevron-shaped arrays of the Cu nano lines. The circular dots in part b are thought to be contaminations.

contamination because they remained discontinuous even after prolonged immersion.

## Discussion

We have for the first time succeeded in forming highly ordered chevron-shaped arrays of continuous copper nano-dot lines, as shown in Figure 3b, by electroless deposition on H-terminated Si(111) surfaces. The success is based on the present finding of the conditions for the preferential deposition of tiny Cu clusters at step sites as well as the preparation of highly ordered step-edge lines by Teflon scratching and  $\text{NH}_4\text{F}$  etching as reported previously.<sup>16,17</sup> As mentioned in the preceding section, the preferential deposition of tiny Cu clusters at step sites occurs when the H–Si(111) wafers are immersed in a deoxygenated neutral aqueous solution of a very low  $\text{Cu}^{2+}$  concentration (less than 10  $\mu\text{M}$ ) with  $\text{pH} \approx 7$ . Why is this

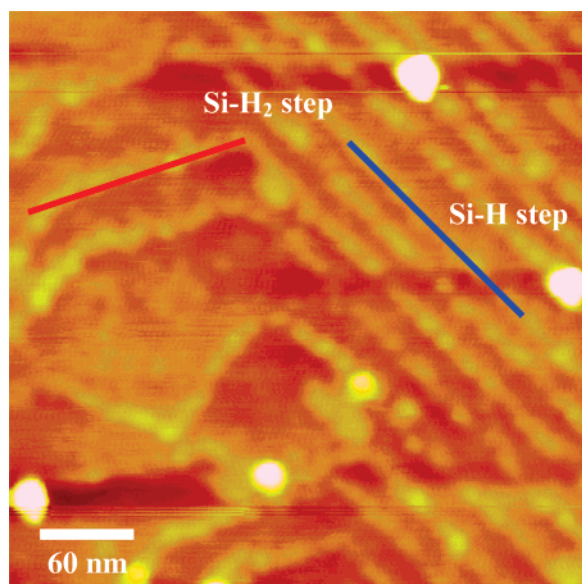
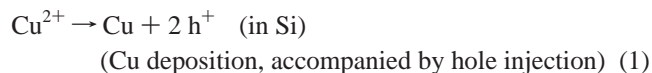


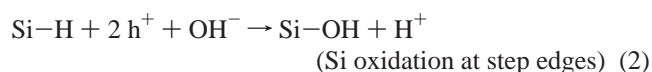
**Figure 4.** AFM image of a H-Si(111) surface on which Cu was deposited by immersion in a deoxygenated aqueous 1  $\mu\text{M}$   $\text{Cu}^{2+}$  solution for 30 s.

condition favorable for the Cu deposition at the step edges? A plausible mechanism might be given as follows:

The electrodeposition of metals and the electroless deposition of metals will proceed by different mechanisms from each other. Let us consider here only the latter mechanism. How does the electroless deposition of Cu on n-Si occur? We have first to note that large upward band bending is present near the n-Si surface when it is in contact with the  $\text{Cu}^{2+}$  solution because the n-Si and the solution should be in electronic equilibrium, namely, the Fermi level of n-Si,  $E_{\text{F}}(\text{n-Si})$ , should agree with the equilibrium redox ( $\text{Cu}^{2+}/\text{Cu}$ ) level,  $eU^{\text{eq}}(\text{Cu}^{2+}/\text{Cu})$ , of the solution (where  $e$  is the elementary charge). Therefore, it is difficult to assume that  $\text{Cu}^{2+}$  reduction occurs by conduction-band electrons of n-Si. In other words, it is most probable that the electroless deposition of Cu proceeds via a hole-injection mechanism (i.e., the  $\text{Cu}^{2+}$  reduction by valence-band electrons), as reported<sup>23</sup> for the electroless deposition of Pt, Au, Ag, and Pd on n-Si



The injected hole may react with water or  $\text{OH}^-$  at step edges



The above argument is supported by the following consideration. The flat-band potential ( $U_{\text{fb}}$ ) of n-Si is reported<sup>24</sup> to be approximately  $-0.58$  V vs SCE (or  $-0.34$  V vs NHE) at  $\text{pH} \approx 7.9$ , and if the energy difference between the Fermi level and the bottom of the conduction band for n-Si is estimated from its resistivity to be  $0.20$  eV, then the conduction- and valence-band edges at the n-Si surface, denoted as  $E_{\text{c}}^{\text{s}}$  and  $E_{\text{v}}^{\text{s}}$ , are calculated to be approximately  $-0.54$  V and  $+0.56$  V vs NHE at  $\text{pH} \approx 7.9$ , respectively. However,  $U^{\text{eq}}(\text{Cu}^{2+}/\text{Cu})$  is estimated to be  $+0.34$  V vs NHE. Thus, the energy difference between  $E_{\text{c}}^{\text{s}}$  and  $eU^{\text{eq}}(\text{Cu}^{2+}/\text{Cu}) = E_{\text{F}}(\text{n-Si})$  (where  $e$  is the elementary charge) is approximately  $0.88$  eV, whereas that between  $E_{\text{v}}^{\text{s}}$  and  $eU^{\text{eq}}(\text{Cu}^{2+}/\text{Cu}) = E_{\text{F}}(\text{n-Si})$  is approximately  $0.22$  eV, and the latter difference is considerably smaller than the former difference.

The resultant Si-OH site at step edges by reaction 2 may undergo further attack of holes and  $\text{OH}^-$ , resulting in step-edge etching. The above-assumed preferential oxidation at the step edges is in harmony with the reported mechanism for the Si etching with  $\text{HF}$ <sup>25</sup> and water,<sup>26,27</sup> in which the oxidation by  $\text{OH}^-$  ions or dissolved  $\text{O}_2$  as the initial step of the etching is assumed to occur more preferentially at step sites than terrace sites. It is also reported<sup>25-27</sup> that the  $\text{OH}^-$  ions attack step Si-H bonds and produce step Si-OH, whereas the dissolved  $\text{O}_2$  causes back-bond oxidation at step Si-Si bonds. In the present work, back-bond oxidation by dissolved  $\text{O}_2$  can be neglected because the used solutions are deoxygenated in all cases.

The next question is how the Cu particles are deposited at step edges. The hole injection is expected to occur not only at step edges but also at terrace sites. Namely, most of Cu adatoms will be formed at the terrace sites. The Cu adatoms at the terrace sites will then diffuse on the terraces and finally be stabilized at the step edges. However, for the high  $\text{Cu}^{2+}$  concentration, the Cu adatoms at the terraces increase in the density and may collide with each other at the terrace before reaching the step edges, forming nuclei for crystal growth at the terrace and finally leading to large Cu dots at the terrace. This argument is supported by the results of Figure 1, in which large Cu dots are produced in a high  $\text{Cu}^{2+}$  concentration of  $1$  mM and the preferential Cu deposition occurs in a low  $\text{Cu}^{2+}$  concentration of  $10$   $\mu\text{M}$ .

Now, let us consider why the Cu adatoms are preferentially stabilized at the step edges. Allongue et al. pointed out<sup>12</sup> that the formation of Si-metal(Au) bonds via Si dangling bonds, formed as an intermediate of the oxidation (etching) reaction at step edges, plays an important role, whereas Tokuda et al. proposed that the interaction between Cu atoms and Si-OH bonds at step edges is an important factor, based on the reported results of the first principles calculation.<sup>28</sup> The results of Figure 4 in the present work show that the Cu particles are adsorbed equally at both the monohydride and the dihydride steps. This result does not necessarily seem to be in harmony with the above explanations, because it is known<sup>29</sup> that the dihydride steps were chemically reactive and more easily etched than the monohydride steps, and therefore it is expected that the Cu deposition should occur more preferentially at the dihydride steps than the monohydride steps. A simpler explanation might be given by considering a larger adsorption energy for the Cu adatoms at the step edges than at the terraces.

Finally, let us consider the pH effect on the Cu deposition. In the preceding section, we mentioned that Cu particles were deposited at the step edges in the nearly neutral and alkaline solutions, whereas in the acidic solution Cu was hardly deposited, though in the alkaline solution the step-edge lines were considerably disturbed. These results can be explained on the basis of the aforementioned hole-injection mechanism for the Cu deposition. As mentioned earlier, the equilibrium redox  $\text{Cu}^{2+}/\text{Cu}$  potential,  $U^{\text{redox}}(\text{Cu}^{2+}/\text{Cu}) = E_{\text{F}}(\text{n-Si})/e$ , is about  $0.22$  V above the surface valence-band edge ( $E_{\text{v}}^{\text{s}}/e$ ) at  $\text{pH} \approx 7.9$ . This implies that the hole-injection process has an activation energy of approximately  $0.22$  eV at  $\text{pH} \approx 7.9$ . It is also known<sup>24</sup> that the flat-band potential and hence  $E_{\text{c}}^{\text{s}}$  and  $E_{\text{v}}^{\text{s}}$  shift downward with decreasing the solution pH, whereas the  $U^{\text{redox}}(\text{Cu}^{2+}/\text{Cu})$  is independent of pH. Thus, the activation energy increases with decreasing pH; namely, the hole injection occurs less efficiently with decreasing pH. We might say that under the experimental conditions in the present work the hole injection is negligible in the acidic solution, occurs slightly in the neutral solution, and is rather efficient in the alkaline solution, which causes little

Cu deposition in the acidic solution, a little and efficient Cu deposition in the neutral and alkaline solutions, respectively, as observed (Figure 2).

It is to be noted that the present experimental results show that sufficiently slow Cu deposition is suitable for the formation of continuous Cu nano-dot lines at step edges, as indicated by the condition that a very low  $\text{Cu}^{2+}$  concentration of  $1\ \mu\text{M}$  is necessary. The condition of a neutral solution of  $\text{pH} \cong 7.9$  comes from the same reason. The rather efficient hole injection together with the high  $\text{OH}^-$  concentration in the alkaline solution will cause effective etching at the step edges, leading to a heavy disturbance at the step-edge lines (Figure 2c) and a decrease in the amount of the deposited Cu particles by peeling off. The above arguments suggest that the formation of well-ordered continuous Cu nano-dot lines at step edges is achieved when the hole injection, the Cu-adatom deposition, and the etching at step edges proceed slowly enough.

## Conclusions

We have investigated electroless deposition of Cu particles on the n-type H-Si(111) surface from deoxygenated aqueous  $\text{Cu}^{2+}$  solutions. The investigations of the influences of the  $\text{Cu}^{2+}$  concentration and the solution pH have revealed that the deposited tiny Cu particles were preferentially formed at step edges under the condition that the  $\text{Cu}^{2+}$  concentration is sufficiently low ( $10\ \mu\text{M}$  or less) and the pH is nearly 7, or in other words, when the hole injection, the Cu-adatom deposition, and the etching at step edges proceed slowly enough. On the basis of this finding and the previously reported novel method to arrange the step-edge lines, we have for the first time succeeded in producing well-ordered chevron-shaped arrays of continuous Cu nano-dot lines on the H-Si(111) surface. The present study provides a new approach to produce ordered nanowires on the Si(111) surface by the chemical, self-organization method.

**Acknowledgment.** This work was partially supported by the Core Research for Evolutional Science and Technology program of the Japan Science and Technology Corporation.

## References and Notes

- (1) *Nanomaterials: Synthesis, Properties, and Applications*; Edelstein, A. S., Cammarata, R. C., Eds.; Institute of Physics: London, 1998.
- (2) *Electrochemistry of Nanomaterials*; Hodes, G., Ed.; Wiley-VCH: Weinheim, Germany, 2001.
- (3) Wilson, M.; Kannangara, K.; Smith, G.; Simmons, M.; Raguse, B.; *Nanotechnology: Basic Science and Emerging Technologies*; Chapman & Hall/CRC: Boca Raton, FL, 2002.
- (4) H. Konoshita. *J. Vac. Sci. Technol., B* **2005**, 23, 2584.
- (5) Marumoto, K.; Yabe, H.; Aya, S.; Kise, K.; Ami, S.; Sasaki, K.; Watanabe, H.; Itoga, K.; Sumitani, H. *J. Vac. Sci. Technol., B* **2003**, 21, 207.
- (6) Gates, B. D.; Xu, Q.; Stewart, M.; Ryan, D.; Willson, C. G.; Whitesides, G. M. *Chem. Rev.* **2005**, 105, 1171.
- (7) Solak, H. H.; He, D.; Li, W.; Cerrina, F. *J. Vac. Sci. Technol., B* **1999**, 17, 3052.
- (8) Hosaka, S.; Hosoki, S.; Hasegawa, T.; Koyanagi, H.; Shintani, T.; Miyamoto, M. *J. Vac. Sci. Technol., B* **1995**, 13, 2813.
- (9) Kolb, D. M.; Ullmann, R.; Ziegler, J. C. *Electrochim. Acta* **1998**, 43, 2751.
- (10) Hara, K.; Ohdomari, I. *Jpn. J. Appl. Phys.* **1998**, 37, L1333.
- (11) Imanishi, A.; Morisawa, K.; Nakato, Y. *Electrochem. Solid-State Lett.* **2001**, 4, C69.
- (12) Munford, M. L.; Maroun, F.; Cortes, R.; Allongue, P.; Pasa, A. A. *Surf. Sci.* **2003**, 537, 95.
- (13) Homma, T.; Wade, C. P.; Chidsey, E. D. *J. Phys. Chem. B* **1998**, 102, 7920.
- (14) Tokuda, N.; Hojo, D.; Yamasaki, S.; Miki, K.; Yamabe, K. *Jpn. J. Appl. Phys.* **2003**, 42, L1210.
- (15) Tokuda, N.; Watanabe, H.; Hojo, D.; Yamasaki, S.; Miki, K.; Yamabe, K. *Appl. Surf. Sci.* **2004**, 237, 528.
- (16) Imanishi, A.; Nagai, T.; Nakato, Y. *J. Phys. Chem. B* **2004**, 109, 21.
- (17) Nagai, T.; Imanishi, A.; Nakato, Y. *Appl. Surf. Sci.* **2004**, 237, 532.
- (18) Kern, W.; Puotinen, D. A. *RCA Rev.* **1970**, 31, 187.
- (19) Higashi, G. S.; Chabal, Y. J.; Trucks, G. W.; Raghavachari, K. *Appl. Phys. Lett.* **1990**, 56, 656.
- (20) Fukidome, H.; Matsumura, M.; Komeda, T.; Namba, K.; Nishioka, Y. *Electrochem. Solid-State Lett.* **1999**, 2, 393.
- (21) Zhou, X.; Ishida, M.; Imanishi, A.; Nakato, Y. *Electrochim. Acta* **2000**, 45, 4655.
- (22) Zhou, X.; Ishida, M.; Imanishi, A.; Nakato, Y. *J. Phys. Chem. B* **2001**, 105, 156.
- (23) Yae, S.; Tanaka, H.; Kobayashi, T.; Fukumuro, N.; Matsuda, H. *Phys. Status Solidi C* **2005**, 2, 3476.
- (24) Nakato, Y.; Ueda, T.; Egi, Y.; Tsubomura, H. *J. Electrochem. Soc.* **1987**, 134, 353.
- (25) Garcia, S. P.; Bao, H.; Hines, M. A. *Surf. Sci.* **2003**, 541, 252.
- (26) Fukidome, H.; Matsumura, M. *Surf. Sci.* **2000**, 463, L649.
- (27) Usuda, K.; Yamada, K. *J. Electrochem. Soc.* **1997**, 144, 3204.
- (28) Tatsumura, K.; Watanabe, T.; Hara, K.; Hoshino, T.; Ohdomari, I. *Phys. Rev. B* **2001**, 64, 115406.
- (29) Flidr, J.; Huang, Y. C.; Hines, M. A. *J. Chem. Phys.* **1999**, 111, 6970.